Infection by *Plasmodium* changes shape and stiffness of hepatic cells

Peter Eaton[a*], Vanessa Zuzarte-Luis[b], Maria M. Mota[b], Nuno C. Santos[c], and Miguel Prudêncio[b]

[a] REQUIMTE/Departamento de Química e Bioquímica, Faculdade de Ciências, Universidade do Porto, Rua do Campo Alegre, 687, 4169-007 Porto, Portugal. E-mail: peter.eaton@fc.up.pt; Fax: +351 220 402 659; Tel: +351 220 402585

[b] Malaria Unit, Instituto de Medicina Molecular, Faculdade de Medicina, Universidade de Lisboa, Portugal

[c] Biomembranes Unit, Instituto de Medicina Molecular, Faculdade de Medicina, Universidade de Lisboa, Portugal

* Corresponding author: (peter.eaton@fc.up.pt)

Short title: *Plasmodium* infection probed by AFM

Keywords: malaria, *Plasmodium*, atomic force microscopy, nanoindentation, liver, hepatic cells

4,651 Words, 4 Figures, 41 References

Abstract

Infection of liver cells by *Plasmodium*, the malaria parasite, is a clinically silent, obligatory step of the parasite's life cycle. We have studied the progression of *Plasmodium* infection in hepatic cells by atomic force microscopy, measuring both topographical and nanomechanical changes upon infection. In recent years, a number of studies have suggested that cellular nanomechanical properties can be correlated with disease progression. Our results show that infected cells exhibit

considerable topographical changes which can be correlated to the presence of the parasite, leading to a significant roughening of the cell membrane. The nanomechanical measurements showed that infected cells were significantly stiffer than noninfected cells. Furthermore, the stiffening of the cells appeared to be a cellular reaction to the *Plasmodium* infection, rather than a result of the stiffness of the invading parasites themselves. This report provides the first evidence of mechanical changes occurring in hepatic cells in response to *Plasmodium* infection.

Malaria is the most important vector-borne disease in the world, threatening ~40% of the human population. It is caused by *Plasmodium*, a protozoan parasite that is transmitted to the host through the bite of an *Anopheles* mosquito. In the mammalian host the infection progresses in two consecutive stages, termed hepatic (or liver) and erythrocytic (or blood) stages. During the first stage, sporozoites injected through skin travel to the liver and infect hepatocytes. Hepatocyte invasion results in the formation of a specialized compartment, the parasitophorous vacuole (PV), inside which *Plasmodium* parasites multiply, generating exoerythrocytic forms (EEFs) [1]. At the end of their development in the liver, *Plasmodium* parasites differentiate into merozoites, which are released into the blood stream inside vesicles called merosomes [2]. This step initiates the blood stage of infection, during which disease symptoms occur. During the liver stage, the intense replication process is accompanied by the significant growth of the EEFs until they eventually take up most of the available intracellular space [3]. This process is probably accompanied by a subversion of host cell resources ensuring the parasite's survival and transmission [4]. Although the mechanisms of parasite growth and replication have been addressed, nothing is known about the nanomechanical properties of infected hepatocytes or about how they are affected by EEF growth. Although clinically silent, the liver stage is an obligatory step for *Plasmodium* infection and, therefore, a crucial determinant of disease progression. The detailed characterization of the host cell responses to the presence of *Plasmodium* parasites will represent a step forward in the development of prophylactic strategies as any changes occurring in the cell at this stage are potential targets for intervention.

Atomic force microscopy (AFM) is a high-resolution imaging technique with particular importance to medicine, since it is capable of imaging in physiological buffers [5]. Furthermore, it allows a wide range of "non-imaging" experiments, further broadening the range of

applications in biomedical science [6, 7]. In particular, nanomechanical measurements have proven useful to characterize a range of pathogens and cells under pathological conditions. An increasing number of diseases are known to change the mechanical properties of the cells and tissues they affect [8]. For example, Cross et al. investigated the nanomechanical properties of metastatic cancer cells and found that the tumor cells were considerably less stiff than normal cells from the same patients [9, 10]. Several other reports have also found cancerous and precancerous cells to have reduced stiffness values [11-14], this is likely because the decreased stiffness and increased deformability aids cancer cells in invading other tissues [15]. It is now well-known that *Plasmodium*-infected erythrocytes are considerably stiffer than non-infected erythrocytes, which may contribute to disease severity by sequestration in microvasculature, and eventual blocking of the venules [16]. However, to the best of our knowledge no work has been described studying the biomechanical properties of *Plasmodium*-infected hepatocytes.

In the present work, we used an established *in vitro* infection system that employs Huh7 cells, a human hepatoma cell line, and the rodent model parasite *Plasmodium berghei* ANKA [17]. In a similar system, EEFs can be detected inside hepatoma cells until ~72 hours post-invasion (hpi) [18], with merosomes starting to bud off infected cells as early as 55 hpi [19]. We studied the growth of the parasite during this stage using AFM. We not only used the imaging capabilities of the AFM to record topographical changes during EEF growth, but also made nanomechanical measurements of the cellular elasticity, in order to determine if mechanical changes occur due to infection. Here, we report on the considerable physical changes that occur in both topography and mechanical properties of the hepatic cells upon *Plasmodium* infection and speculate on the molecular bases of these alterations.

Methods

Parasites, cells and infection

Huh7 cells, a human hepatoma cell line, were infected by GFP-expressing *P. berghei* ANKA sporozoites[20]. Further details are given in the Supplementary Materials.

Cell imaging

Cells for imaging in air were prepared by removing the culture medium at selected time points and washing twice with PBS prior to fixation with 4% paraformaldehyde for 10 min at room temperature. Coverslips containing the fixed cells were washed twice with PBS, then with cell culture grade H_2O to remove any traces of salt, and allowed to dry in air. Cells for imaging in liquid were prepared simply by replacing the culture medium with fresh medium.

Atomic force microscopy

All AFM experiments were carried out using a Nanowizard II AFM (JPK Instruments) integrated with a Zeiss Axiovert 200 observer inverted optical microscope. Imaging was carried out in two conditions: on fixed, dried cells in air, and on unfixed living cells in liquid. Under all conditions, the green fluorescence from the GFP-expressing parasite was used to distinguish infected from non-infected cells. Data were analyzed by Rq measurements and feature counting, as described in the Supplementary materials. Live cells were imaged and probed in fresh growth medium, at 37ºC, using a JPK BioCell module. Further details of AFM imaging and nanoindentation measurements on live cells are given in the Supplementary materials.

Results

Infected cells present topographic differences when compared to non-infected cells

Aiming to use the nanoscale measurement capabilities of AFM to determine whether any changes occur in the morphology and mechanical properties of hepatic cells upon *Plasmodium* infection, we initially carried out imaging experiments on fixed cells. Since the occurrence of infected cells in unsorted samples was very low, we used GFP-expressing parasites, and a combined epifluorescence and AFM to identify this subpopulation (Figure 1).

One of the first features to be noticed is that in the region where the EEF is present, we often found a large raised area of the membrane, which could be distinguished from the rest of the infected cell and became increasingly visible throughout the time of infection. Furthermore, in samples from 48 hpi onwards, the surface texture seems also quite different, with a number of raised features present on the membrane over the EEF location (highlighted in figure 1C). While such features are also seen in non-infected cells, their frequency in infected cells was higher. In addition, non-infected cells show several pit-like depressed features, which were less frequently observed in infected cells. As shown in figures 1B, 1C and 1D, the change in texture of the membrane, as well as the large raised area over the EEF, became increasingly visible throughout the time of infection. At 24 hpi, the fluorescence signal from the parasite was considerably smaller than at the later time points, and not all cells (ca. 80%) examined by AFM showed visible features on the membrane that could be correlated with the location of the PV, as seen in the epifluorescence microscope. At later time points, however, the location of the PV was obvious in the AFM images, appearing as a distinct raised area co-localized with the fluorescence signal. After around 72 hpi, a high degree of differentiation could be observed on

these features (figure 1D, 1E). This may correspond to the merozoite-filled vesicles that form during the final phases of parasite replication. These vesicles will eventually exit the hepatic cells as merosomes, each containing hundreds or thousands of merozoites [21]. It was interesting to note that on occasions this splitting of the parasitic vacuole could apparently be seen clearly in the AFM images while it was not visible in the epifluorescence images (for example, see figure 1E).

Altogether, these AFM images suggest that parasite development indeed alters the topography of the host cell. In order to quantify these effects, we measured a texture parameter that would be sensitive to such changes, namely membrane roughness, R_q. Furthermore, we counted the number of raised and lowered features (<2 μm^2 in area) on the infected and noninfected cell surfaces (figure 2B). The analysis showed that roughness increased considerably for infected cells from approximately 48 hpi onwards, while it did not change for non-infected cells (Figure 2A). Data in Figure 2B confirm that these small raised features increased in number with time. This may partly explain the roughness increase at these later time-points, although it should be remembered that roughness parameters will also include contributions from other cell surface features.

While AFM imaging of fixed cells provides considerably higher contrast and finer details than imaging of unfixed, live cells [5, 22], the uncertainty about the relevance of the features seen in more physiologically relevant conditions, means that the features seen on dried and fixed cells must be interpreted with care. Thus, next we attempted to image living hepatoma cells (Supporting Information Figures S1 and S2). Unfortunately, as has been found elsewhere, the image quality achieved in liquid was far lower than that on fixed and dried cells, and images of

living cells show very few membrane details since membranes are too flexible to be imaged by mechanical means [22]. Thus, we could not confirm the observations made on fixed cells.

Infection by *Plasmodium* changes the stiffness of hepatic cells

The results obtained with fixed cells strongly suggest that the development of the parasite affects the host cell membrane morphology. We hypothesized that this could be related to physical changes that occur due to the growth of this very large foreign body within the cell. As such, we sought to determine whether this results in nanomechanical differences in the infected cells and, to that end, we performed indentation analysis on cells at 24 and 48 hpi. Cells were probed for a maximum of 2 h to ensure that cell viability was maintained throughout the experimental procedure. The overall results, comparing infected and noninfected cells are summarized in figure 3, which gives the mean and standard deviation values of the Young's modulus of the cells obtained by fitting the nanoindentation curves as described in the methods section. Young's modulus is a measurement of sample stiffness, assuming that the sample (hepatic cells) can be treated as an elastic material.

The results show that while no significant differences could be detected between the infected and uninfected cells at 24 hpi, infected cells 48 hpi displayed significantly higher Young's modulus values relative to uninfected cells at this time (4.7×; $p < 0.0001$; Figure 3). It is worth noting that the variation in the measurements on cells 48 hpi is quite high. In fact, the standard deviation in the Young's modulus was 30-50% of the mean value in all cases *except* in the case of cells analyzed 48 hpi, where a very large variation (140 % of the mean value) was found. In particular,

it was seen that several curves gave extremely high values of E, (>1 kPa), indicating stiffness values increased by up to 10 times relative to the control.

In addition, we made measurements in selected regions of the cells. For the infected cells, a set of data was collected over the area containing the EEFs (as revealed by the green fluorescence), so that we were pressing onto the membrane directly above the parasitic vacuole, and another set of data was measured on the same (infected) cell, but on a region of the membrane away from the parasitophorous vacuole. In parallel, we collected data for non-infected cells at each of the selected time points (Figure 4).

The data in Figure 4 show that considerable differences were found between different regions on the infected cells. At 24 hpi, the membrane above the infected cell body was somewhat stiffer than the area above the parasites. Although the difference was not large (127 Pa (cell) *versus* 93 Pa (EEF)), it was significant ($p = 0.007$). This contrasts with the results obtained by combining all the data on the infected cell (figure 3), where at 24 hpi no significant differences could be observed. At 48 hpi, the stiffness values showed a much greater difference between the values measured on the membrane over the cell and the membrane over the EEF. In this case, the mean values were very different (819 Pa for the cell versus 211 Pa for the EEF), and the difference was highly significant ($p<0.0001$). It is clear that the data at 24 hpi largely overlapped in terms of stiffness, while great differences were found after 48 hpi (figure 4B, C). In this set of data, it can be seen that there was a large number of measurements which found the cells to be greatly stiffer than the uninfected cells, and also stiffer than the area of the membrane measured directly above the EEF, while there still existed a population of measurement with relatively low stiffness.

Discussion

In considering the meaning of these results, two trends stand out. Firstly, increased stiffness (i.e higher values of E) seemed to occur when measuring the membrane over the main body of the cell, rather than directly over the area containing the EEFs. Secondly, there is a very large spread in the values of the Young's modulus values found at 48 hpi. Cell stiffness and structure are mainly dependent on the three components that collectively make up the cytoskeleton, i.e., microtubules, intermediate filaments, and actin filaments. These fibers vary greatly in their elastic moduli, persistence lengths and dimensions, and they can be heterogeneously distributed throughout the cell at the nanoscale [15, 23]. Indeed, it is known that AFM can probe subsurface structures in living mammalian cells. For example, using force volume imaging, Smith et al. showed that much higher stiffness was recorded over actin stress fibers despite the presence of the cell membrane covering the entire cell [24]. It is possible to use a similar technique to measure the mechanical properties of actin stress fibers inside the cell [25]. In fact, we can verify this effect by looking at the imaging results shown in figures 1A, S1 and S2 (supporting information). As seen in figure 1, the surface of the cell is rather flat, not showing the sort of linear features typically associated with the cytoskeleton components, particularly actin stress fibers. In fact, on dried and fixed cells, such features were seen very rarely. This was because the membrane had been stiffened by the fixing procedure. On the other hand, the unfixed, living cells often showed long, straight features, apparently higher than the surrounding material (see figures S1 and S2 in the supporting information).

These features are likely due to the cell cytoskeleton, and the reason they appear in these images is because they are considerably stiffer than the membrane. Thus, cytoskeleton features are visible when the membrane is flexible (unfixed), but not when it is stiff (fixed). It is common to see the cytoskeleton when carrying out contact mode imaging on living cells [7], and the visibility of the actin fibers increases with increasing applied force [26]. In the nanoindentation experiments reported here (figures 3 and 4), in the case of the infected cells, measurements were made in two locations: directly over the PV, and over the central part of the cell membrane, away from the PV, but we did not control the measurement positions in regard to positions of structures such as stress fibers. Therefore, when applying nanoindentation experiments, some results would probably be obtained directly over cytoskeleton fibers close to the membrane surface. This can go some way to explaining the very large variation in all the nanoindentation results.

To the best of our knowledge, there are no reports on the effect of physical force arising from the growth of *Plasmodium* EEFs within hepatocytes by any technique. It is known that cells can regulate their cytoskeleton based on either external or internal forces, which leads to the reorganisation of the filaments within the cytoskeleton network [23]. Therefore it seems plausible that the changes seen in nanoindentation results at 48 hpi were in fact due to changes in cytoskeleton structure brought about by internal forces applied to the cell structure by the rapidly growing parasite. Confocal microscopy analysis of the distribution of actin, one of the cystoskeleton components, in infected cells at approximately 24 and 48 hpi time-points (Supporting Information Figure S3), did not show any visible change in actin fibers in the infected cells. However, the changes induced by physical forces can take place in other ways,

such as other cytoskeletal component reinforcement , cytoplasm stiffening , or the number of cytoskeleton binding sites can be altered [25, 27]. In a recent study, changes in cell stiffness that occur through the progression of ovarian cancer, which were measured by AFM, were shown to be related to cytoskeletal rearrangement[14]. Therefore, although we could detect no actin growth in the infected cells by confocal microscopy, we speculate that the remarkable change in mechanical properties after 48 h infection by *P. berghei* was most likely due to cytoskeleton remodeling, which was either too subtle to be observed with the confocal microscope, or not based on actin growth (i.e., either microtubule, intermediate filament or focal adhesion-based).

As far as the topographical changes observed are concerned, it would seem likely that they may also be based on the physical forces exerted by the cell. While it may be that the membrane depressions seen predominantly away from the EEF were fenestrae, which are naturally present on the cell membrane[28], the origin of the raised features is less clear. Attempts to observe these in living cells were ambiguous, although some raised features with similar dimensions were occasionally observed (Supporting Information Figure S2). One reason could be that these features occur more frequently in regions of membrane stress, which appear more in regions where the membrane was experiencing additional forces due to PV growth. Another alternative could be that these are features that also occur in the living cells (as occasionally observed by AFM imaging of living cell membranes) and that the altered cellular metabolism that results from the parasites' growth [4] has an effect on the regulation of features such as ventricles and endo- and exocytosis, giving rise to the changes seen in infected cells. However, a possible artifact due to cell fixation cannot be ruled out, such as membrane blistering caused by the paraformaldehyde fixative action on the membrane, which is known to occur on some cells with

aldehyde fixing procedures [29]. One effect that was very clear from the AFM imaging studies was that of the PV separating itself into merosomes at late time-points. The fact that the AFM is able to observe the process of formation of the merozoites without the use of fluorescence indicates that AFM could be applied to observe this effect in case where staining or expression of fluorescent proteins is undesirable. Further, due to the higher resolution of AFM, it may be able to measure finer details of the process than those accessible by fluorescence-based techniques.

Conclusions

The topographic imaging experiments showed differences in cell morphology between infected and noninfected cells. On the other hand, the nanoindentation data obtained on live cells clearly showed that that approximately 48 h after infection by *Plasmodium berghei*, hepatoma cells increased greatly in stiffness. The spatially-resolved data acquisition showed us that the increased stiffness in the infected cells did not come from direct measurements of the growing EEFs within the cell. Instead, this result was an indirect effect of the presence of the parasites; i.e., it was a cellular response to infection, indicating that the cell changes its mechanical properties when infected by *Plasmodium*. This increase was accompanied by a large increase in the standard deviation, suggesting that the stiffening occurs in cytoskeleton components. This is the first evidence of the mechanical pressure exerted by *Plasmodium* parasitophorous vacuole growth on liver cells during infection. The work described in this report also underlines the great potential atomic force microscopy has as a nanotechnology-based tool for unraveling cellular and subcellular details in disease progression, not just in terms of topography but also in nanomechanical properties.

Acknowledgements

The authors would like to thank Ana Serra-Caetano for her kind assistance with the fluorescence activated cell sorting procedure. Thanks are also due to Maria José Feio for help with the figures.

References

1. Prudencio M, Rodriguez A, Mota MM. The silent path to thousands of merozoites: the Plasmodium liver stage. Nature Reviews Microbiology 2006; 4(11): 849-856.
2. Sturm A, Amino R, van de Sand C, Regen T, Retzlaff S, Rennenberg A, et al. Manipulation of host hepatocytes by the malaria parasite for delivery into liver sinusoids. Science 2006; 313(5791): 1287-1290.
3. Silvie O, Mota MM, Matuschewski K, Prudencio M. Interactions of the malaria parasite and its mammalian host. Current Opinion in Microbiology 2008; 11(4): 352-359.
4. Albuquerque SS, Carret C, Grosso AR, Tarun AS, Peng X, Kappe SHI, et al. Host cell transcriptional profiling during malaria liver stage infection reveals a coordinated and sequential set of biological events. BMC Genomics 2009; 10: 270.
5. Eaton P, West P. Atomic Force Microscopy. Oxford: OUP. 2010, 256.
6. Muller DJ, Dufrene YF. Atomic force microscopy as a multifunctional molecular toolbox in nanobiotechnology. Nat Nano 2008; 3(5): 261-269.
7. Ikai A, A Review on: Atomic Force Microscopy Applied to Nano-mechanics of the Cell, *Nano/Micro Biotechnology*, Berlin: Springer-Verlag Berlin; 2010. p. 47-61.
8. Suresh S, Spatz J, Mills JP, Micoulet A, Dao M, Lim CT, et al. Connections between single-cell biomechanics and human disease states: gastrointestinal cancer and malaria. Acta Biomaterialia 2005; 1(1): 15-30.
9. Cross SE, Jin YS, Tondre J, Wong R, Rao J, Gimzewski JK. AFM-based analysis of human metastatic cancer cells. Nanotechnology 2008; 19(38).
10. Cross SE, Jin YS, Rao J, Gimzewski JK. Nanomechanical analysis of cells from cancer patients. Nature Nanotechnology 2007; 2(12): 780-783.
11. Billingsley DJ, Kirkham J, Bonass WA, Thomson NH. Atomic force microscopy of DNA at high humidity: irreversible conformational switching of supercoiled molecules. Physical Chemistry Chemical Physics 2010; 12(44): 14727-14734.
12. Lekka M, Laidler P, Gil D, Lekki J, Stachura Z, Hrynkiewicz AZ. Elasticity of normal and cancerous human bladder cells studied by scanning force microscopy. European Biophysics Journal with Biophysics Letters 1999; 28(4): 312-316.
13. Leporatti S, Vergara D, Zacheo A, Vergaro V, Maruccio G, Cingolani R, et al. Cytomechanical and topological investigation of MCF-7 cells by scanning force microscopy. Nanotechnology 2009; 20(5): 055103.

14. Ketene AN, Schmelz EM, Roberts PC, Agah M. The Effects of Cancer Progression on the Viscoelasticity of Ovarian Cell Cytoskeleton Structures. Nanomedicine: Nanotechnology, Biology and Medicine; In Press, Accepted Manuscript.
15. Suresh S. Biomechanics and biophysics of cancer cells. Acta Biomaterialia 2007; 3(4): 413-438.
16. Marinkovic M, Diez-Silva M, Pantic I, Fredberg JJ, Suresh S, Butler JP. Febrile temperature leads to significant stiffening of Plasmodium falciparum parasitized erythrocytes. American Journal of Physiology-Cell Physiology 2009; 296(1): C59-C64.
17. Prudencio M, Rodrigues CD, Ataide R, Mota MM. Dissecting in vitro host cell infection by Plasmodium sporozoites using flow cytometry. Cellular Microbiology 2008; 10(1): 218-224.
18. Prudencio M, Derbyshire ET, Marques CA, Krishna S, Mota MM, Staines HM. Plasmodium berghei-infection induces volume-regulated anion channel-like activity in human hepatoma cells. Cellular Microbiology 2009; 11(10): 1492-1501.
19. Labaied M, Jayabalasingham B, Bano N, Cha S-J, Sandoval J, Guan G, et al. Plasmodium salvages cholesterol internalized by LDL and synthesized de novo in the liver. Cellular Microbiology 2011; 13(4): 569-586.
20. Franke-Fayard B, Trueman H, Ramesar J, Mendoza J, van der Keur M, van der Linden R, et al. A Plasmodium berghei reference line that constitutively expresses GFP at a high level throughout the complete life cycle. Molecular and Biochemical Parasitology 2004; 137(1): 23-33.
21. Sturm A, Amino R, van de Sand C, Regen T, Retzlaff S, Rennenberg A, et al. Manipulation of Host Hepatocytes by the Malaria Parasite for Delivery into Liver Sinusoids. Science 2006; 313(5791): 1287-1290.
22. Murphy MF, Lalor MJ, Manning FCR, Lilley F, Crosby SR, Randall C, et al. Comparative study of the conditions required to image live human epithelial and fibroblast cells using atomic force microscopy. Microscopy Research and Technique 2006; 69(9): 757-765.
23. Fletcher DA, Mullins D. Cell mechanics and the cytoskeleton. Nature 2010; 463(7280): 485-492.
24. Smith BA, Tolloczko B, Martin JG, Grütter P. Probing the Viscoelastic Behavior of Cultured Airway Smooth Muscle Cells with Atomic Force Microscopy: Stiffening Induced by Contractile Agonist. Biophysical Journal 2005; 88(4): 2994-3007.
25. Watanabe-Nakayama T, Machida S-i, Harada I, Sekiguchi H, Afrin R, Ikai A. Direct Detection of Cellular Adaptation to Local Cyclic Stretching at the Single Cell Level by Atomic Force Microscopy. Biophysical Journal 2011; 100(3): 564-572.
26. Radmacher M, Studying the Mechanics of Cellular Processes by Atomic Force Microscopy, in W. YuLi and E.D. Dennis, Editors *Methods in Cell Biology* Academic Press; 2007. p. 347-372.
27. Matthews BD, Overby DR, Mannix R, Ingber DE. Cellular adaptation to mechanical stress: role of integrins, Rho, cytoskeletal tension and mechanosensitive ion channels. Journal of Cell Science 2006; 119(3): 508-518.
28. Horn T, Christoffersen P, Henriksen JH. Alcoholic liver injury: Defenestration in noncirrhotic livers—a scanning electron microscopic study. Hepatology 1987; 7(1): 77-82.

29. Shelton E, Mowczko WE, Scanning electron microscopy of membrane blisters produced by glutaraldehyde fixation and stablised by postfixation in Osmium Tetroxide, in J.E. Rash and C.S. Hudson, Editors *Freeze Fracture Methods, Artifacts and Interpretations*, New York: Raven Press; 1979. p. 67-69.

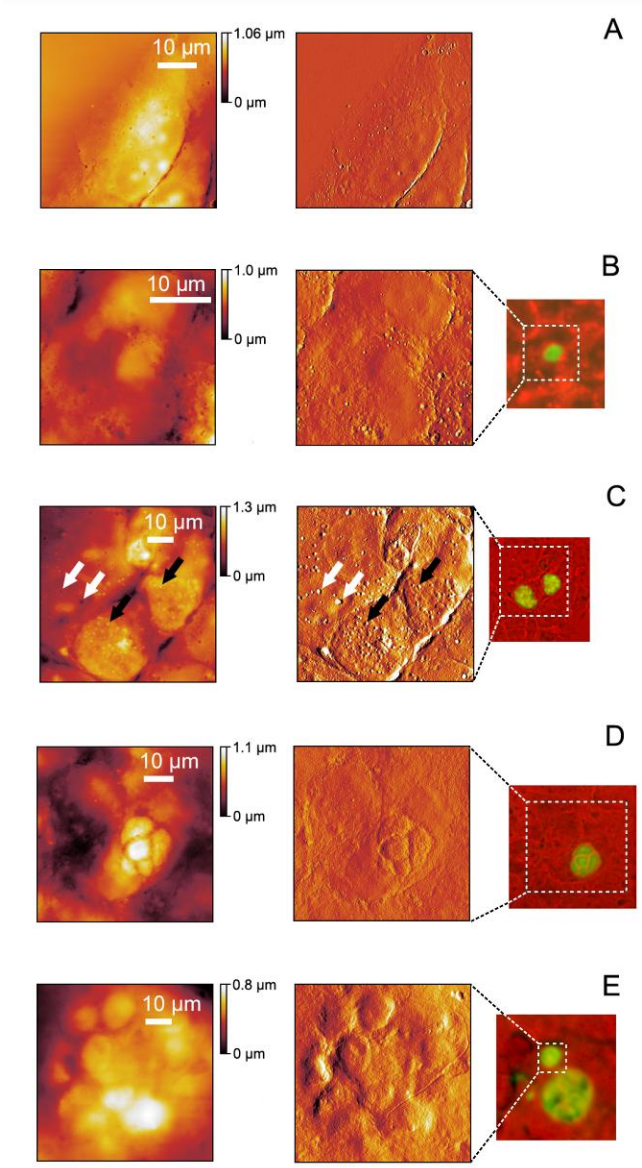

Figure 1. Representative images of dried and fixed hepatoma cells. A: AFM image of uninfected cell (left: height image; right: amplitude image). B, C, D and E: AFM height (left) and amplitude (center), with corresponding epifluorescence (right) images of infected cells fixed 24 (B), 48 (C) 72 (D) and 72 (E) h post-infection with GFP-expressing *P. berghei* parasites (phase contrast images of cells are red channel, GFP channel is green). The white arrows in the 48 hour image highlight lowered features in uninfected cells and the black arrows raised features above the location of EEFs.

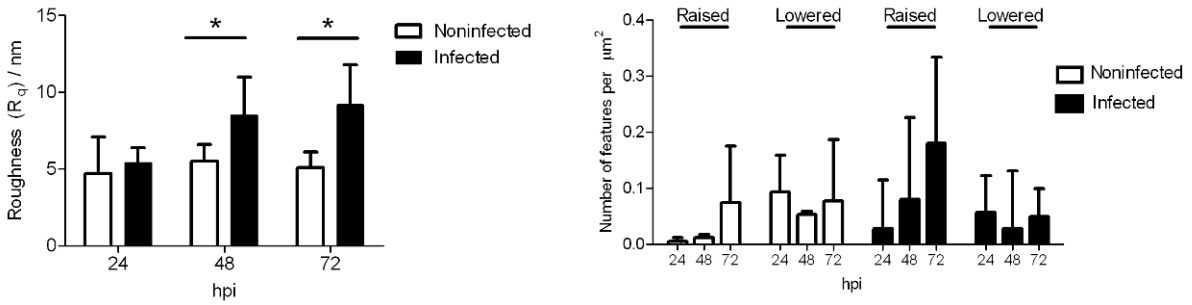

Figure 2. Morphology parameters measured on fixed and dried cells. A: roughness values. Means of all measured values are shown. The starred pairs were found to be significantly different ($p < 0.05$) in the infected and noninfected cells. B: density of raised and lowered features counted on cell surfaces. Error bars represent the standard deviation.

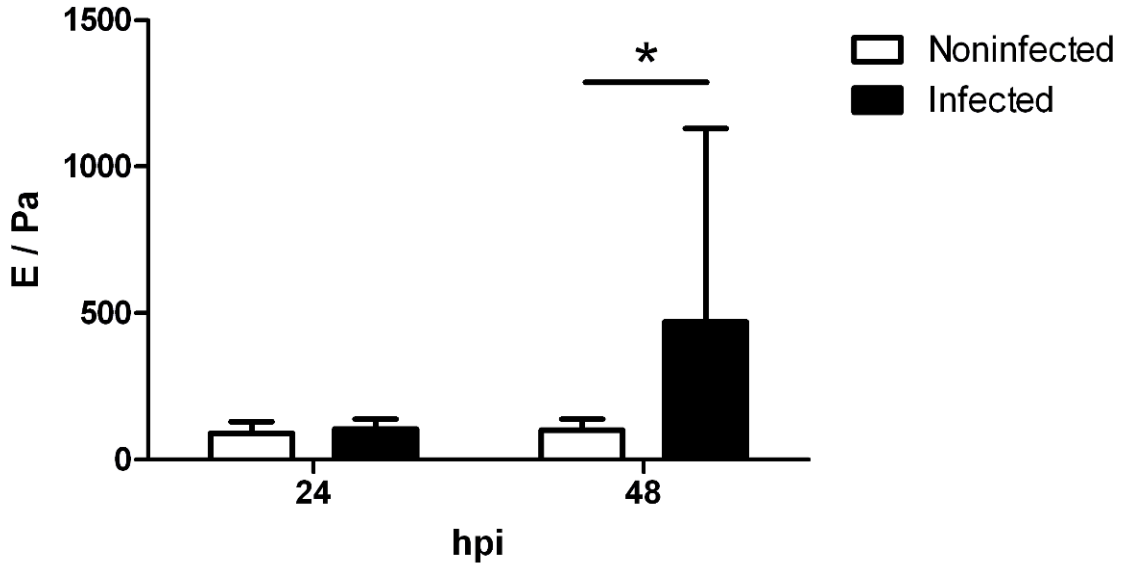

Figure 3. Overall nanoindentation results. All measurements are Young's Modulus (E) expressed in Pascals, and are the results of modelling as described in the text. The error bars represent the standard deviation of the plotted means. Starred data pairs are significantly different ($p<0.05$).

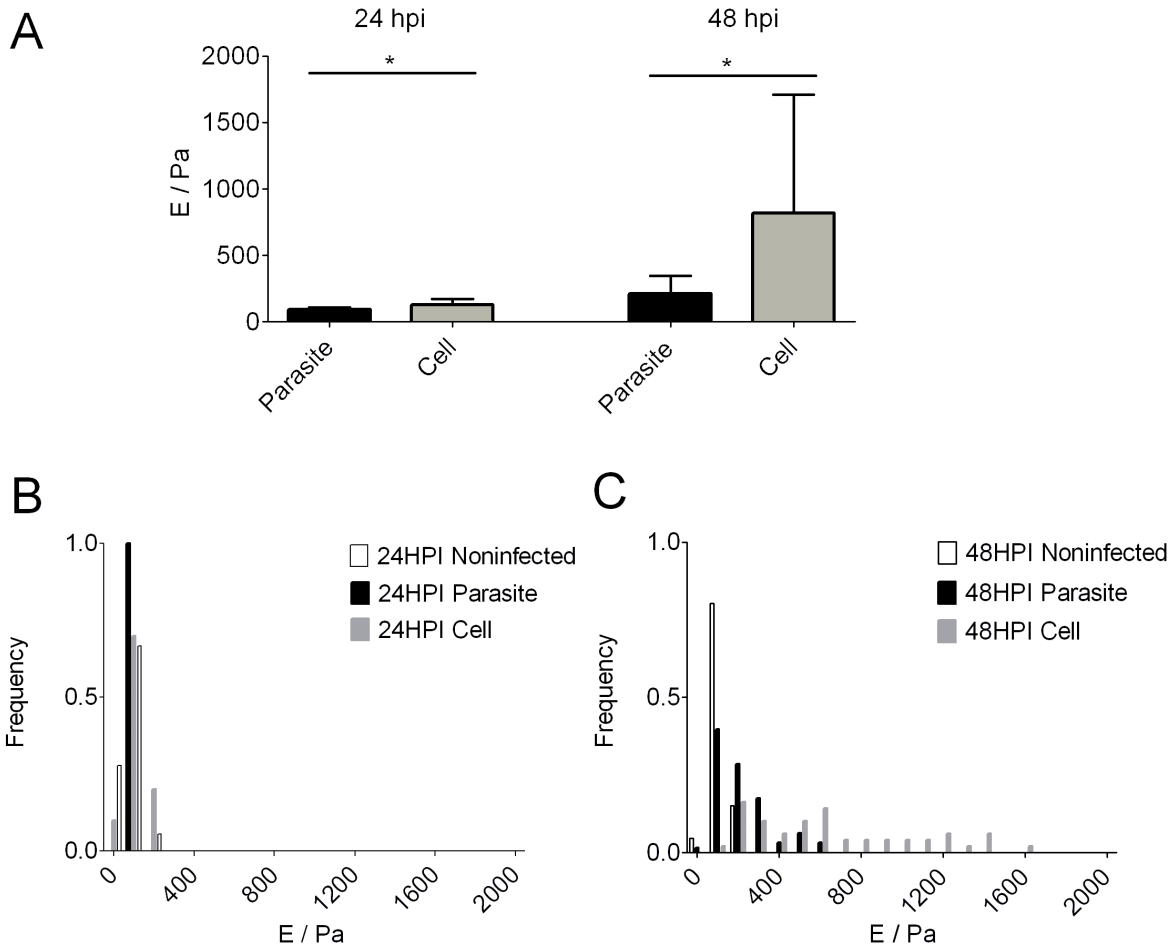

Figure 4. A: Results of nanoindentation comparing results on infected cells measured directly over the parasite location (EEF) and over the main body of the cell. Starred pairs were significantly different ($P<0.05$). B and C: histograms illustrating the distribution of values obtained for Young's modulus by nanoindentation measurements on cells 24 (A) and 48 (B) hpi.